Phase field crystal based prediction of temperature and density dependence of elastic constants through a structural phase transition

Mark Ainsworth and Zhiping Mao

Phys. Rev. B **100**, 104101 — Published 3 September 2019

DOI: 10.1103/PhysRevB.100.104101

Phase Field Crystal Based Prediction of Temperature and Density Dependence of Elastic Constants Through Structural Phase Transition*

Mark Ainsworth† and Zhiping Mao†
Division of Applied Mathematics, Brown University, 182 George St, Providence RI 02912, USA.
(Dated: August 20, 2019)

Explicit, analytical forms are obtained for the elastic constants arising from the PFC model in which the dependence of the constants on proxies for the temperature and density in the PFC model is clearly exhibited. The expressions indicate that the elastic constants are multi-valued in certain temperature ranges corresponding to regions where two or more phases co-exist, in agreement with experimental observations.

The analytical formulae for the variation of the elastic constants with *density* agree with those obtained using a computational approach in [1] but only in certain regimes. Specifically, if it is assumed that only the body centered cubic state is present, then our formulae agree with the numerical results presented in [1]. In general, the Bcc state is not the only phase present and, if other phases are taken into account, then the results differ in those regions where alternative states are favoured energetically. Similar conclusions hold if one looks at temperature dependence instead of density variation.

Keywords: Elastic constant. Phase Field Crystal. Poisson ratio.

I. INTRODUCTION

The modelling of ordered structures using the phase field crystal approach in the pioneering work of Elder and Grant [2, 3] has attracted considerable attention as an effective technique for capturing the complex spatial structures and phase transitions which previously could only be observed using an atomistic level model. Early successes of the model included the prediction of the phase diagram, grain boundary energies consistent with the Reed-Shockley law amongst many others.

Despite the fact that the elastic properties have been studied right from the earliest works on the PFC model, it was only relatively recently [1] pointed out that the evaluation of the elastic constants must take pre-existing strains into account. In particular, in [1] it was shown that one can achieve this by constructing a new thermodynamic formulation to incorporate the pre-stressed state in both solid and liquid phases through either a generalized Gibbs free energy or a via new finite strain tensor if using the Helmholtz free energy. Examples given in [1] make use of a numerical optimisation based approach for obtaining the elastic constants from the PFC model.

The current work aims to obtain explicit, analytical forms for the elastic constants arising from the PFC model in which the dependence of the constants on proxies for the temperature and density in the PFC model is clearly exhibited. While the variation of the elastic constants with temperature is only to be expected, the behaviour of the elastic constants in certain temperature ranges may come as a surprise to some. For example, results reported in [4] for $LiKSO_4$ (reproduced here in Figure 1) show that the elastic constants C_{11}, C_{12} and C_{44} are multi-valued in certain temperature ranges. Although we do not attempt to model $LiKSO_4$ here, the analytical formulae we obtain for the elastic constants predicted by the PFC model considered in [1] are also

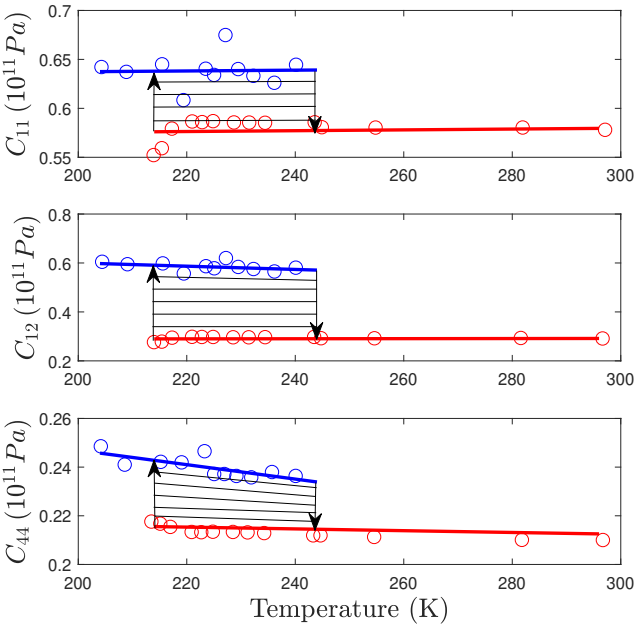

FIG. 1: Elastic constants C_{11}, C_{12} and C_{44} against temperature for $LiKSO_4$. The circles are the experimental values; the solid lines represent the linear fits to the data. See also [4, Figures 2-3].

* This work was supported by the MURI/ARO on "Fractional PDEs for Conservation Laws and Beyond: Theory, Numerics and Applications" (W911NF-15-1-0562). This work was also supported in part by the DOE PhILMs project (No. de-sc0019453).
† Corresponding authors.

found to be multi-valued in certain temperature ranges corresponding to regions where two or more phases co-exist.

The analytical result we obtain for the variation of the elastic constants with *density* agree with those obtained using a computational approach in [1] but only in certain regimes. In particular, if one restricts attention to the body centered cubic state, then our formulae are in agreement with the numerical results presented in [1] across the full range. However, if one takes into account the existence of other phases then the results differ in those regions where the Bcc state is not energetically favoured. Moreover, as with the temperature variation, it is shown that the explicit expressions predict multi-valued elastic constants in regions of co-existence.

Finally, we investigate what the explicit formulae have to say about the Poisson's ratio. Simple manipulations of the expressions leads to the conclusion that the Poisson ratio predicted using the PFC model should lie in the range $[1/3, 1/2)$ for Bcc, $[1/4, 1/2)$ for hexagons and $[0, 1/2)$ for stripes.

II. PHASE FIELD CRYSTAL MODEL

We consider the usual free energy functional for the phase field crystal (PFC) model [2, 3]:

$$\mathcal{F}(\phi) = \int_\Omega \left\{ \frac{\phi}{2}\left[\lambda(q_0^2 + \nabla^2)^2\right]\phi + F(\phi) \right\} d\boldsymbol{r}$$

with the function $F(\phi)$ given by

$$F(u) = a\phi + \frac{b}{2}\phi^2 + \frac{g}{4}\phi^4,$$

where the order-parameter $\phi(\boldsymbol{r})$ is a measure of the crystal density field measured from some constant reference value ρ_0, namely, $\phi(\boldsymbol{r}) = \rho(\boldsymbol{r}) - \rho_0$ with $\rho(\boldsymbol{r})$ being the density, and λ, q_0, a, b and g are phenomenological parameters. The wavenumber q_0 determines the magnitude $|\boldsymbol{K}_i|$ of the principal reciprocal lattice vectors that correspond to the first peak of the liquid structure factor [3]. The parameters λ and b can be selected by fitting the functional $b + \lambda(q_0^2 + \nabla^2)^2$ to the first order peak in experimental measurements of the structure factor. Typically, the linear and cubic terms $a\phi$, ϕ^3 appearing in the free energy (1) are omitted [1, 5]. However, it has been shown in [1] that the linear term plays crucial role in determining the pre-existing pressure of the system and hence on the calculation of elastic constants, and we shall therefore retain the term.

The dimensionless free energy functional [1]

$$\mathcal{F}(\varphi(\boldsymbol{r})) = \int_\Omega \left\{ \gamma\varphi + \frac{\varphi}{2}\left[-\epsilon + (1+\nabla^2)^2\right]\varphi + \frac{1}{4}\varphi^4 \right\} d\boldsymbol{r} \tag{1}$$

is obtained by applying the affine transformations

$$q_0\boldsymbol{r} \to \boldsymbol{r},\ \sqrt{g/\lambda q_0^4}\phi \to \varphi,\ \frac{g}{\lambda^2 q_0^4}\mathcal{F} \to \mathcal{F},$$

with the dimensionless parameters given by

$$\gamma = \frac{a}{q_0^6}\sqrt{g/\lambda^3},\ \epsilon = -\frac{b}{\lambda q_0^4}.$$

For an elastic deformation with strain $\boldsymbol{\varepsilon}$, the total number of particles

$$N = \int_\Omega \rho(\boldsymbol{r})d\boldsymbol{r} = \bar{\rho}|\Omega|$$

remains constant, and hence the relationship

$$\bar{\rho}_{\boldsymbol{\varepsilon}} = \frac{|\Omega_0|}{|\Omega_{\boldsymbol{\varepsilon}}|}\bar{\rho}_0 \tag{2}$$

holds between the average density of the strained system and that of the unstrained system. Here $|\Omega_0|$ and $|\Omega_{\boldsymbol{\varepsilon}}|$ are the undeformed and deformed volumes, respectively, which are related according to the equation

$$|\Omega_{\boldsymbol{\varepsilon}}| = det[\boldsymbol{I} + \boldsymbol{\varepsilon}] \cdot |\Omega_0| \tag{3}$$

with $\boldsymbol{I}$ being the second-order unit tensor and $\boldsymbol{\varepsilon}$ being the strain. In turn $\bar{\varphi}_0$ and $\bar{\varphi}_{\boldsymbol{\varepsilon}}$, satisfy the following relation [1]:

$$\bar{\varphi}_{\boldsymbol{\varepsilon}} = \frac{|\Omega_0|}{|\Omega_{\boldsymbol{\varepsilon}}|}(\bar{\varphi}_0 + \tilde{\rho}_0) - \tilde{\rho}_0, \tag{4}$$

where $\tilde{\rho}_0 = \sqrt{g/(\lambda q_0^4)}\rho_0$.

The phase field crystal model can be viewed as the gradient flow in H^{-1} associated with the above free energy functional so that the dynamics, in the conservative sense, are given by

$$\frac{\partial\varphi}{\partial t} = \nabla \cdot \left(\nabla \frac{d\mathcal{F}}{d\varphi}\right)$$

resulting in a dimensionless partial differential equation (PDE)

$$\partial_t\varphi - \Delta\left((1+\nabla^2)^2\varphi + f(\varphi)\right) = 0, \tag{5}$$

where $f(\varphi) = \varphi^3 - \epsilon\varphi + \gamma$.

III. FORMATION OF ORDERED STRUCTURES AND PHASE DIAGRAM

A key feature of the equation (5) is the existence of ordered structure phases or, *pattern formation* [6–8]. One of the main ideas behind PFC modeling is to interpret these patterns as corresponding to different physical phases (liquid, different crystalline structures, ...).

In this section, we briefly describe the pattern formation. To this end, one looks for non-trivial solutions to (5) in the form

$$\varphi(\boldsymbol{r}, t) = \bar{\varphi}(t) + \sum_{\boldsymbol{K}} A_{\boldsymbol{K}}(t)e^{\mathrm{i}\boldsymbol{K}\cdot\boldsymbol{r}}, \tag{6}$$

where $\boldsymbol{K}$ is the (nonzero) reciprocal lattice vector and $A_{\boldsymbol{K}}$ is the corresponding Fourier-component amplitude with $A_{-\boldsymbol{K}} = A^*_{\boldsymbol{K}}$. The issue then becomes one of determining the lattice vector and the amplitudes.

One approach [1] uses direct numerical minimisation of the free energy

$$F_0 = \min_{\{A_{\boldsymbol{K}}\},\{\boldsymbol{K}\}} \mathcal{F}(\{A_{\boldsymbol{K}}\},\{\boldsymbol{K}\},\bar{\varphi},|\Omega|)$$

with fixed $\bar{\varphi}$ and Ω. The resulting minimizers give the total energy as well as the amplitude $\{A_{\boldsymbol{K}}\}$ of the unstrained state, but do not necessarily satisfy the equation (5). Instead, we pursue an alternative approach to obtain steady state solutions, whereby we derive the amplitudes equation for different types of pattern, and then solve to obtain explicit expressions for the steady states which satisfy equation (5).

A. Pattern formation

The standard approach for identifying two dimensional structures consists of seeking non-trivial solutions to (5) of the form

$$\begin{aligned}\varphi(\boldsymbol{r},t) =& A_1(t)e^{\mathrm{i}\boldsymbol{k}_1\cdot\boldsymbol{r}} + A_2(t)e^{\mathrm{i}\boldsymbol{k}_2\cdot\boldsymbol{r}} \\ &+ A_3(t)e^{\mathrm{i}\boldsymbol{k}_3\cdot\boldsymbol{r}} + c.c. + \bar{\varphi}(t),\end{aligned} \tag{7}$$

where c.c. denotes the complex conjugate and

$$\boldsymbol{k}_1 = \boldsymbol{v},\ \boldsymbol{k}_2 = \boldsymbol{R}\boldsymbol{k}_1,\ \boldsymbol{k}_3 = \boldsymbol{R}\boldsymbol{k}_2$$

with $\boldsymbol{R}$ denoting a rotation by $2\pi/3$ and $\boldsymbol{v}$ is an arbitrary fixed orientation e.g. $\boldsymbol{v} = (1,0)$. By substituting the Ansatz (6) into (5) and comparing coefficients of the modes $e^{\mathrm{i}\boldsymbol{k}_j\cdot\boldsymbol{r}}, j = 1,2,3$, one obtains the following equations [9] for the amplitudes in (6):

$$\begin{aligned}\partial_t A_1 =& \big((\epsilon - 3\bar{\varphi}^2)A_1 - 6\bar{\varphi}A_2^*A_3^* \\ &- A_1(3|A_1|^2 + 6|A_2|^2 + 6|A_3|^2)\big), \\ \partial_t A_2 =& \big((\epsilon - 3\bar{\varphi}^2)A_2 - 6\bar{\varphi}A_3^*A_1^* \\ &- A_2(3|A_2|^2 + 6|A_3|^2 + 6|A_1|^2)\big), \\ \partial_t A_3 =& \big((\epsilon - 3\bar{\varphi}^2)A_3 - 6\bar{\varphi}A_1^*A_2^* \\ &- A_3(3|A_3|^2 + 6|A_1|^2 + 6|A_2|^2)\big),\end{aligned} \tag{8}$$

together with the following equation for the evolution of $\bar{\varphi}(t)$:

$$\frac{d\bar{\varphi}(t)}{dt} = 0.$$

The simplest non-zero solution of the form (6) is obtained by taking

$$A_1(t) = A_2(t) = A_3(t) = 0.$$

This solution shows no spatial structure and is therefore interpreted as the *liquid phase*.

In addition to the liquid phase, the amplitude equations possess two distinct types of spatially structured solutions: *stripes*, that are invariant under the translation $x_2 \to x_2 + const$; and *hexagons*, that are invariant under rotation by $\pm 2\pi/3$.

For the stripe solutions, one seeks a non-trivial solution of the form (6) with

$$A_1(t) = A_s(t) \neq 0,\ A_2(t) = A_3(t) = 0.$$

The amplitude equations then reduce to the single equation

$$\partial_t A_s = (\epsilon - 3\bar{\varphi}^2)A_s - 3|A_s|^2 A_s,$$

which has a trivial stationary solution $A_s(t) = 0$ and two nontrivial stable stationary solutions in which

$$A_s(t) = A_\pm = \pm\sqrt{(\epsilon - 3\bar{\varphi}^2)/3},\ \epsilon \geq 3\bar{\varphi}^2. \tag{9}$$

Turning now to hexagonal patterns one seeks a solution of the form (6) with

$$A_1(t) = A_2(t) = A_3(t) = A_h(t) \neq 0.$$

The amplitude equations (8) then reduce to a single equation of the form

$$\partial_t A_h = (\epsilon - 3\bar{\varphi}^2)A_h - 6\bar{\varphi}A_h^2 - 15A_h^3,$$

which has a trivial (unstable) solution $A_h(t) = 0$ and two nontrivial (stable) stationary solutions:

$$A_h(t) = A_\pm = -\frac{1}{5}\bar{\varphi} \pm \frac{1}{15}\sqrt{15\epsilon - 36\bar{\varphi}^2},\ \epsilon \geq \frac{36}{15}\bar{\varphi}^2. \tag{10}$$

Here, the + (resp. −) sign is chosen when $\bar{\varphi}$ is negative (resp. positive).

In addition, one can also obtain a non-trivial three dimensional structure, body-centered cubic (Bcc) steady state, in the form

$$\begin{aligned}\varphi(\boldsymbol{r},t) =& \bar{\varphi}(t) + 4A_b(t)\big(\cos(qx)\cos(qy) \\ &+ \cos(qy)\cos(qz) + \cos(qz)\cos(qx)\big),\end{aligned}$$

where $q = 1/\sqrt{2}$. Substituting the above expression into the free energy functional (1) yields the following amplitude equation for A_b corresponding to the Bcc

$$\partial_t A_b = (\epsilon - 3\bar{\varphi}^2)A_b - 12\bar{\varphi}A_b^2 - 45A_b^3,$$

which has a trivial (unstable) solution $A_b(t) = 0$ and two nontrivial (stable) stationary solutions:

$$A_b(t) = A_\pm = -\frac{2}{15}\bar{\varphi} \pm \frac{1}{15}\sqrt{5\epsilon - 11\bar{\varphi}^2},\ \epsilon \geq \frac{11}{5}\bar{\varphi}^2. \tag{11}$$

Here, the + (resp. −) sign is chosen when $\bar{\varphi}$ is negative (resp. positive).

B. Phase diagram

The question as to which of the solutions given above is preferred leads to the study of the phase diagram [10]. To this end, we compute the free energy densities $f = \mathcal{F}/|\Omega|$ of each kind of patterns.

The total energy of the steady states is obtained by substituting the steady state solutions into the free energy functional (1), namely,

$$F_0 = \mathcal{F}(\varphi_0(\boldsymbol{r})),$$

where $\varphi_0(\boldsymbol{r})$ is a steady state solution. In particular, we are interested in the constant state,

$$\varphi_c(\boldsymbol{r}) = \bar{\varphi};$$

the stripe state

$$\varphi_s(x) = A_s \cos(x) + \bar{\varphi};$$

the hexagon state

$$\varphi_h(x,y) = 2A_h\left(\cos x + 2\cos(x/2)\cos(\sqrt{3}y/2)\right) + \bar{\varphi},$$

and; the Bcc state

$$\begin{aligned}\varphi_b(x,y,z) = 4A_b\big(&\cos(qx)\cos(qy)\\ &+\cos(qy)\cos(qz)+\cos(qz)\cos(qx)\big)+\bar{\varphi}\end{aligned}$$

with $q = 1/\sqrt{2}$.

Substituting these states into the dimensionless free energy functional (1) yields the free energy density for: the constant phase

$$f_c(\bar{\varphi}) = \gamma\bar{\varphi} + \frac{1-\epsilon}{2}\bar{\varphi}^2 + \frac{\bar{\varphi}^4}{4}; \tag{12}$$

the stripe phase

$$\begin{aligned}f_s(\bar{\varphi},A_s) =&\frac{1}{2\pi}\int_0^{2\pi}\Phi(\varphi_s)dx\\ =&\gamma\bar{\varphi}+\frac{1-\epsilon}{2}\bar{\varphi}^2+\frac{\bar{\varphi}^4}{4}-\epsilon A_s^2+3\bar{\varphi}^2A_s^2+\frac{3}{2}A_s^4,\end{aligned} \tag{13}$$

where

$$\Phi(\varphi) = \gamma\varphi + \frac{\varphi}{2}(1+\nabla^2)^2\varphi - \frac{\epsilon}{2}\varphi^2 + \frac{\varphi^4}{4}; \tag{14}$$

the hexagon phase

$$\begin{aligned}f_h(\bar{\varphi},A_h) =&\frac{\sqrt{3}}{4\pi^2}\int_0^{\frac{2\pi}{\sqrt{3}}}\int_0^{2\pi}\Phi(\varphi_h)dxdy\\ =&\gamma\bar{\varphi}+\frac{1-\epsilon}{2}\bar{\varphi}^2+\frac{\bar{\varphi}^4}{4}\\ &-3\epsilon A_h^2+9\bar{\varphi}^2A_h^2+12\bar{\varphi}A_h^3+\frac{45}{2}A_h^4,\end{aligned} \tag{15}$$

and; the Bcc phase

$$\begin{aligned}f_b(\bar{\varphi},A_b) =&\frac{\sqrt{2}}{32\pi^3}\int_0^{\frac{4\pi}{\sqrt{2}}}\int_0^{\frac{4\pi}{\sqrt{2}}}\int_0^{\frac{4\pi}{\sqrt{2}}}\Phi(\varphi_b)dxdydz\\ =&\gamma\bar{\varphi}+\frac{1-\epsilon}{2}\bar{\varphi}^2+\frac{\bar{\varphi}^4}{4}\\ &-6\epsilon A_b^2+18\bar{\varphi}^2A_b^2+48\bar{\varphi}A_b^3+135A_b^4.\end{aligned} \tag{16}$$

Applying the Maxwell equal-area construction rule [11] gives the phase diagram shown in Figure 2.

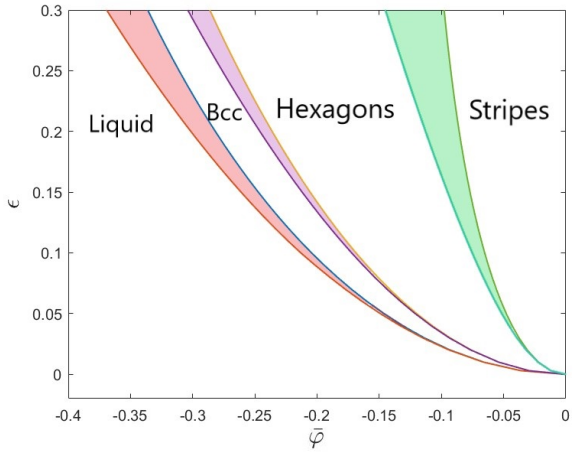

FIG. 2: Phase diagram for the steady states (12)-(16). Shaded areas correspond to regions where two states can co-exist.

IV. ELASTIC CONSTANTS

Consider a system originally in an unstrained state with volume Ω_0 and average density ρ_0. The system is then subjected to a strain $\boldsymbol{\varepsilon}$ resulting in the system having density $\rho_{\boldsymbol{\varepsilon}}$ and volume $\Omega_{\boldsymbol{\varepsilon}}$ given by (2) and (3), and order parameter $\bar{\varphi}_{\boldsymbol{\varepsilon}}$ given by (4). Traditionally, the elastic constants have been computed using the expression

$$C_{ijkl} = \frac{1}{|\Omega_0|}\frac{\partial^2 F(\bar{\varphi}_{\boldsymbol{\varepsilon}},|\Omega_{\boldsymbol{\varepsilon}}|)}{\partial\varepsilon_{ij}\partial\varepsilon_{kl}}\Big|_{\boldsymbol{\varepsilon}=0}. \tag{17}$$

However, as discussed in [1], the above formula is only valid when there is no *pre-existing pressure* in the initial undeformed state. If this is not the case, then it has been shown in [1] that the elastic constants are determined by the Gibbs free energy

$$G(\bar{\varphi}_{\boldsymbol{\varepsilon}},|\Omega_{\boldsymbol{\varepsilon}}|) = F(\bar{\varphi}_{\boldsymbol{\varepsilon}},|\Omega_{\boldsymbol{\varepsilon}}|) + P_0(\bar{\varphi}_{\boldsymbol{\varepsilon}})\cdot|\Omega_{\boldsymbol{\varepsilon}}|, \tag{18}$$

which takes account of the pre-existing pressure of the initial undeformed state

$$P_0(\bar{\varphi}_{\boldsymbol{\varepsilon}}) = -\frac{1}{|\Omega_0|}\frac{\partial F(\bar{\varphi}_{\boldsymbol{\varepsilon}},|\Omega_{\boldsymbol{\varepsilon}}|)}{\partial\varepsilon_{ii}}\Big|_{\boldsymbol{\varepsilon}=0}. \tag{19}$$

The elastic constants are then given by the expression:

$$C_{ijkl} = \frac{1}{|\Omega_0|}\frac{\partial^2 G(\bar{\varphi}_{\boldsymbol{\varepsilon}}, |\Omega_{\boldsymbol{\varepsilon}}|)}{\partial\varepsilon_{ij}\partial\varepsilon_{kl}}\Big|_{\boldsymbol{\varepsilon}=0}. \tag{20}$$

Our objective here is to obtain closed form expressions for the elastic constants with the dependence on the temperature and density given explicitly. The free energy F_0 of the unstrained state takes the form

$$F_0 = \mathcal{F}(\varphi_0(\boldsymbol{r})) = |\Omega_0| \cdot f, \tag{21}$$

where f is given by one of f_c, f_s f_h or f_b, i.e., equations (12), (13), (15) and (16). For the strained state, the free energy is given by

$$F_{\boldsymbol{\varepsilon}} = \min_{\{A_{\boldsymbol{K}}\}} \mathcal{F}(\varphi_{\boldsymbol{\varepsilon}}(\boldsymbol{r})) = \min_{\{A_{\boldsymbol{K}}\}} \mathcal{F}(\{A_{\boldsymbol{K}}\}, \{\boldsymbol{K}_{\boldsymbol{\varepsilon}}\}, \bar{\varphi}_{\boldsymbol{\varepsilon}}, |\Omega_{\boldsymbol{\varepsilon}}|), \tag{22}$$

where $\boldsymbol{K}_{\boldsymbol{\varepsilon}}$ is the strained reciprocal lattice vector given by

$$\boldsymbol{K}_{\boldsymbol{\varepsilon}} = (\boldsymbol{I} + \boldsymbol{\varepsilon})^{-1}\boldsymbol{K}_0.$$

A direct calculation, detailed in the Appendix, yields explicit expressions for the amplitudes $\{A_{\boldsymbol{K}}\}$ of the strained state as well as the first order derivative with respect to the strain $\boldsymbol{\varepsilon}$, i.e., $\frac{\partial A_{\boldsymbol{K}}}{\partial\varepsilon_{ij}}$, see equation (A.9). Moreover, one finds that (see (A.2))

$$\frac{\partial\bar{\varphi}_{\boldsymbol{\varepsilon}}}{\partial\varepsilon_{ii}}\Big|_{\boldsymbol{\varepsilon}=0} = -(\bar{\varphi}_0 + \tilde{\rho}_0), \tag{23}$$

To ease the notation in what follows, we shall not exhibit explicitly that these quantities are understood as being evaluated at $\boldsymbol{\varepsilon} = 0$. Likewise, closed forms of the elastic constants can be obtained by using equations (18)-(22); again details are pronounced in the Appendix.
Stripe State:

$$P_0 = -f_s - \frac{\partial\bar{\varphi}_{\boldsymbol{\varepsilon}}}{\partial\varepsilon_{11}}\left(6A_s^2\bar{\varphi}_0 + \gamma + (1-\epsilon)\bar{\varphi}_0 + \bar{\varphi}_0^3\right) \tag{24}$$

and elastic constants

$$C_{11} = 8A_s^2 + \frac{\partial\bar{\varphi}_{\boldsymbol{\varepsilon}}}{\partial\varepsilon_{11}}\Big(\frac{\partial\bar{\varphi}_{\boldsymbol{\varepsilon}}}{\partial\varepsilon_{11}}\big(1 + 6A_s^2 - \epsilon + 3\bar{\varphi}_0^2\big) + 12A_s\bar{\varphi}_0\frac{\partial A_s^{\boldsymbol{\varepsilon}}}{\partial\varepsilon_{11}}\Big) \tag{25}$$

and

$$C_{12} = \frac{\partial\bar{\varphi}_{\boldsymbol{\varepsilon}}}{\partial\varepsilon_{11}}\Big(\frac{\partial\bar{\varphi}_{\boldsymbol{\varepsilon}}}{\partial\varepsilon_{22}}\big(1 + 6A_s^2 - \epsilon + 3\bar{\varphi}_0^2\big) + 12A_s\bar{\varphi}_0\frac{\partial A_s^{\boldsymbol{\varepsilon}}}{\partial\varepsilon_{22}}\Big), \tag{26}$$

where $\frac{\partial\varphi_{\boldsymbol{\varepsilon}}}{\partial\varepsilon_{ii}}$ is given by (23), A_s is the unstrained stripe amplitude given by (9) and $\frac{\partial A_s^{\boldsymbol{\varepsilon}}}{\partial\varepsilon_{ii}}$ is the first-order derivative of the strained striped amplitude given by (A.9).
Hexagonal State:

$$P_0 = -f_h - \frac{\partial\bar{\varphi}_{\boldsymbol{\varepsilon}}}{\partial\varepsilon_{ii}}\left(12A_h^3 + 18A_h^2\bar{\varphi}_0 + \gamma + (1-\epsilon)\bar{\varphi}_0 + \bar{\varphi}_0^3\right), \tag{27}$$

and elastic constants

$$C_{11} = 9A_h^2 + \frac{\partial\bar{\varphi}_{\boldsymbol{\varepsilon}}}{\partial\varepsilon_{11}}\Big(\frac{\partial\bar{\varphi}_{\boldsymbol{\varepsilon}}}{\partial\varepsilon_{11}}\big(1 + 18A_h^2 - \epsilon + 3\bar{\varphi}_0^2\big) + 36\frac{\partial A_h^{\boldsymbol{\varepsilon}}}{\partial\varepsilon_{11}}(A_h\bar{\varphi}_0 + A_h^2)\Big) \tag{28}$$

and

$$C_{12} = 3A_h^2 + \frac{\partial\bar{\varphi}_{\boldsymbol{\varepsilon}}}{\partial\varepsilon_{11}}\Big(\frac{\partial\bar{\varphi}_{\boldsymbol{\varepsilon}}}{\partial\varepsilon_{22}}\big(1 + 18A_h^2 - \epsilon + 3\bar{\varphi}_0^2\big) + 36\frac{\partial A_h^{\boldsymbol{\varepsilon}}}{\partial\varepsilon_{22}}(A_h\bar{\varphi}_0 + A_h^2)\Big). \tag{29}$$

The elastic constant C_{44} vanishes for both stripes and hexagons.
Body Centered Cubic State:

$$P_0 = -f_b - \frac{\partial\bar{\varphi}_{\boldsymbol{\varepsilon}}}{\partial\varepsilon_{ii}}\left(48A_b^3 + 36A_b^2\bar{\varphi}_0 + \gamma + (1-\epsilon)\bar{\varphi}_0 + \bar{\varphi}_0^3\right), \tag{30}$$

and elastic constants

$$C_{11} = 8A_b^2 + \frac{\partial\bar{\varphi}_{\boldsymbol{\varepsilon}}}{\partial\varepsilon_{11}}\Big(\frac{\partial\bar{\varphi}_{\boldsymbol{\varepsilon}}}{\partial\varepsilon_{11}}\big(1 + 36A_b^2 - \epsilon + 3\bar{\varphi}_0^2\big) + 72\frac{\partial A_b^{\boldsymbol{\varepsilon}}}{\partial\varepsilon_{11}}(A_b\bar{\varphi}_0 + 2A_b^2)\Big) \tag{31}$$

and

$$C_{12} = 4A_b^2 + \frac{\partial\bar{\varphi}_{\boldsymbol{\varepsilon}}}{\partial\varepsilon_{11}}\Big(\frac{\partial\bar{\varphi}_{\boldsymbol{\varepsilon}}}{\partial\varepsilon_{22}}\big(1 + 36A_b^2 - \epsilon + 3\bar{\varphi}_0^2\big) + 72\frac{\partial A_b^{\boldsymbol{\varepsilon}}}{\partial\varepsilon_{22}}(A_b\bar{\varphi}_0 + 2A_b^2)\Big) \tag{32}$$

and

$$C_{44} = 4A_b^2, \tag{33}$$

where A_b is the unstrained Bcc amplitude given by (11).

Observe in each case, the obtained elastic constants are *independent* of the linear term in the free energy functional, i.e., the value of the parameter γ [1].

V. INTERPRETATION OF THE RESULTS

A. Relationship with Experimental Observations

One expects the elastic constants to vary with the temperature, a fact which is also confirmed by experiment, e.g. [4, 12–15]. Less obvious perhaps, but nevertheless also confirmed by experimental observation [4, Figures 2-3] is that the elastic constants are *multi-valued in the co-existing region between two states*. What do the analytic formulas for the elastic constants derived earlier have to say in this case? Figures 3, 4 and 5 contain plots of the elastic constants C_{11}, C_{12} and C_{44} against the value of the value of $-\epsilon$ (corresponding to temperature) across phase transitions. In particular, we observe from Figures

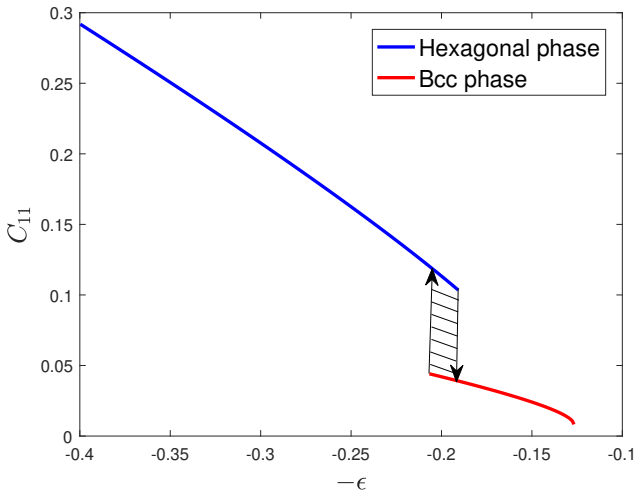

FIG. 3: Variation of the elastic constant C_{11} against the value of $-\epsilon$ corresponding to the temperature. $\bar{\varphi} = -0.24$, $\tilde{\rho}_0 = 0.251$.

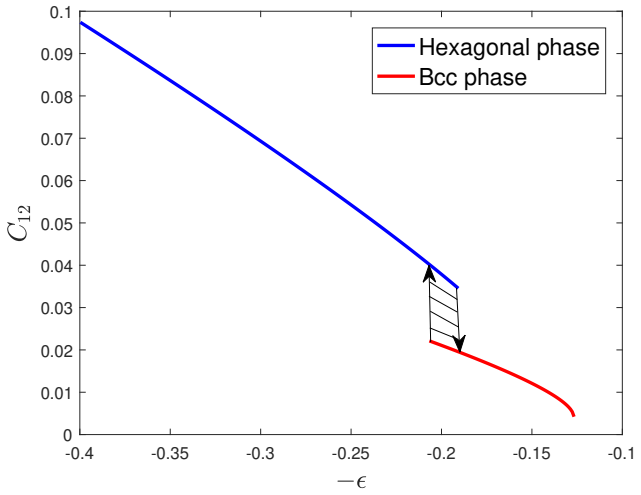

FIG. 4: Variation of the elastic constant C_{12} against the value of $-\epsilon$ corresponding to the temperature. $\bar{\varphi} = -0.24$, $\tilde{\rho}_0 = 0.251$.

3-4 the multi-valued nature of the elastic constants C_{11} and C_{12} in the coexistence regions.

Similarly, one can also consider how the elastic constants depend on the average of density. Figure 6, Figure 7 and Figure 8 show the elastic constants C_{11}, C_{12} and C_{44}, respectively. Again, we observe that the elastic constants are multi-valued in region where phases co-exist.

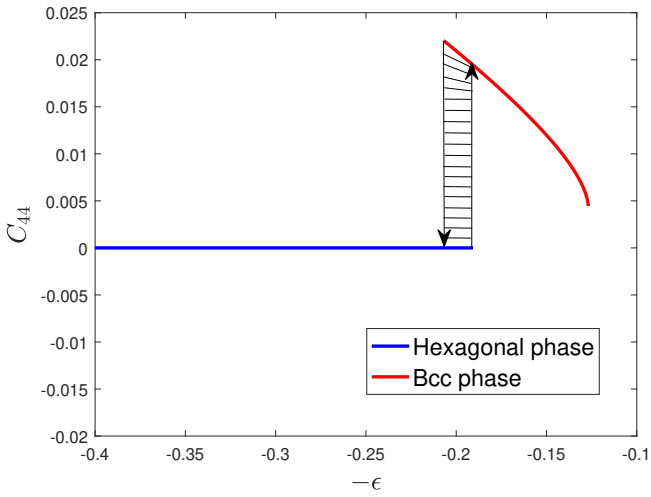

FIG. 5: Variation of the elastic constant C_{44} against the value of $-\epsilon$ corresponding to the temperature. $\bar{\varphi} = -0.24$, $\tilde{\rho}_0 = 0.251$.

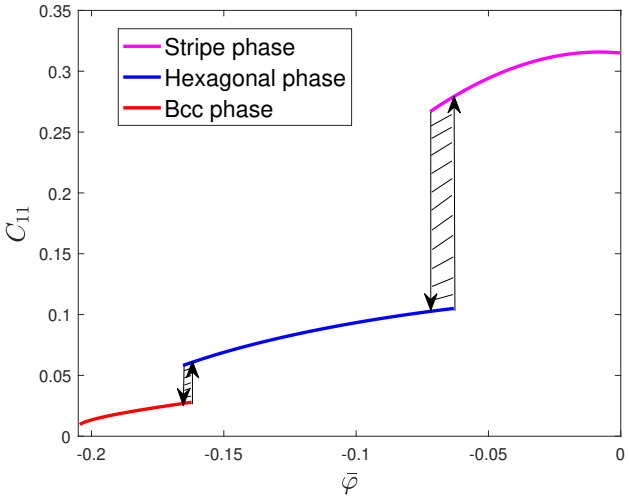

FIG. 6: Variation of the elastic constant C_{11} against the average of the density $\bar{\varphi}$. $\epsilon = 0.0923$, $\tilde{\rho}_0 = 0.251$.

B. Relationship with Existing Work

In [1], the elastic constants were computed using a direct computational minimisation of the free energy in which one first minimizes the free energy $\mathcal{F}$ numerically to determine the equilibrium unstrained state, then applies various strains in a range from -3% to 3% to the equilibrium state and minimizes the free energy again using the corresponding strained values of $\boldsymbol{K}_{\boldsymbol{\varepsilon}}$, $|\Omega_{\boldsymbol{\varepsilon}}|$ and $\bar{\varphi}_{\boldsymbol{\varepsilon}}$, and finally using equations (19)-(20) and the fitting first- and second-order derivatives of $F(\boldsymbol{\varepsilon})$ with respect to ε_{ij}. Figure 9 compares the results of the present work

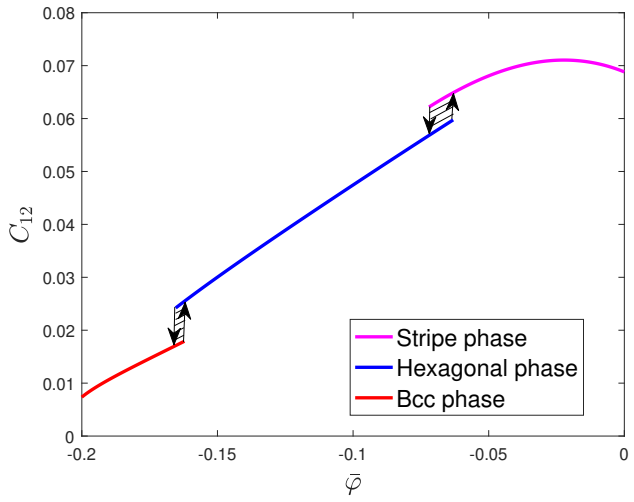

FIG. 7: Variation of the elastic constant C_{12} against the average of the density $\bar{\varphi}$. $\epsilon = 0.0923$, $\tilde{\rho}_0 = 0.251$.

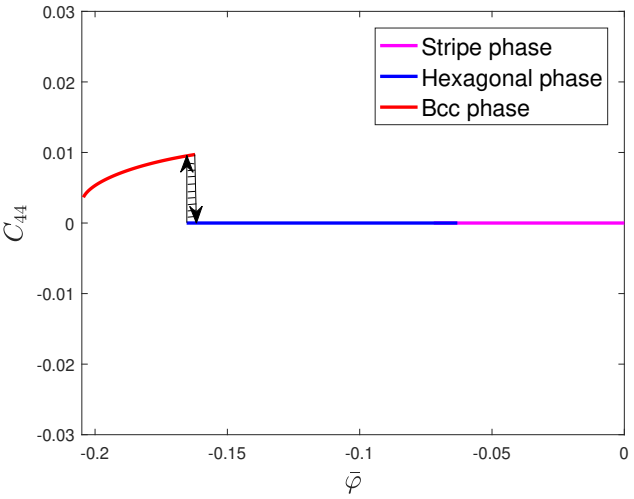

FIG. 8: Variation of the elastic constant C_{44} against the average of the density $\bar{\varphi}$. $\epsilon = 0.0923$, $\tilde{\rho}_0 = 0.251$.

with those given in [1] for the pressure and elastic constants C_{11}, C_{12} and C_{44}. Observe that the results are consistent with one another if one uses the expressions (30)-(33) for the pressure and the elastic constants for the Bcc phase across *all densities*. However, as shown in Section III, phase changes occur at certain densities and temperatures. Taking the phase changes into account results in multi-valued expressions which, it seems, are not readily obtained using the direct numerical simulation.

C. Explicit Expression for Poisson's Ratio

A drawback of the classical PFC approach is that the Poisson's ratio is *always* given by 1/3. However, the arguments used in this work lead to analytical expressions for the Poisson's ratio which show that (for the Bcc state) Poisson's ratio varies between 1/3 and 1/2. In particular, since $\frac{\partial\bar{\varphi}_{\boldsymbol{\varepsilon}}}{\partial\varepsilon_{11}} = \frac{\partial\bar{\varphi}_{\boldsymbol{\varepsilon}}}{\partial\varepsilon_{22}}$ and $\frac{A_b^{\boldsymbol{\varepsilon}}}{\partial\varepsilon_{11}} = \frac{\partial A_b^{\boldsymbol{\varepsilon}}}{\partial\varepsilon_{22}}$ as $\boldsymbol{\varepsilon} \to 0$, using the equation (31) and (32), the Poisson's ratio for the Bcc state is given by

$$\nu = \frac{C_{12}}{C_{11}+C_{12}} = \frac{4A_b^2+a}{12A_b^2+2a}, \tag{34}$$

where

$$a = \frac{\partial\bar{\varphi}_{\boldsymbol{\varepsilon}}}{\partial\varepsilon_{11}}\Big(\frac{\partial\bar{\varphi}_{\boldsymbol{\varepsilon}}}{\partial\varepsilon_{11}}\big(1+36A_b^2-\epsilon+3\bar{\varphi}_0^2\big)+72\frac{\partial A_b^{\boldsymbol{\varepsilon}}}{\partial\varepsilon_{11}}\big(A_b\bar{\varphi}_0+2A_b^2\big)\Big). \tag{35}$$

Similarly, we can show that the Poisson's ratio for the hexagons

$$\nu = \frac{C_{12}}{C_{11}+C_{12}} = \frac{3A_h^2+a}{12A_h^2+2a},$$

where

$$a = \frac{\partial\bar{\varphi}_{\boldsymbol{\varepsilon}}}{\partial\varepsilon_{11}}\Big(\frac{\partial\bar{\varphi}_{\boldsymbol{\varepsilon}}}{\partial\varepsilon_{11}}\big(1+18A_h^2-\epsilon+3\bar{\varphi}_0^2\big)+36\frac{\partial A_h^{\boldsymbol{\varepsilon}}}{\partial\varepsilon_{11}}\big(A_h\bar{\varphi}_0+A_h^2\big)\Big), \tag{36}$$

or for the stripes

$$\nu = \frac{C_{12}}{C_{11}+C_{12}} = \frac{a}{8A_s^2+2a},$$

where

$$a = \frac{\partial\bar{\varphi}_{\boldsymbol{\varepsilon}}}{\partial\varepsilon_{11}}\Big(\frac{\partial\bar{\varphi}_{\boldsymbol{\varepsilon}}}{\partial\varepsilon_{11}}\big(1+6A_s^2-\epsilon+3\bar{\varphi}_0^2\big)+12A_s\bar{\varphi}_0\frac{\partial A_s^{\boldsymbol{\varepsilon}}}{\partial\varepsilon_{11}}\Big), \tag{37}$$

We show in Figure 10 the value of a for all states. Observe that we have nonnegative value of a for most of the region of solid (stripe, hexagon and Bcc) (hatched region). By providing that $a \geq 0$, we have for the Bcc state,

$$\nu - \frac{1}{3} = \frac{a}{36A_b^2+6a} \geq 0, \quad \nu - \frac{1}{2} = \frac{-A_b^2}{6A_b^2+a} < 0,$$

i.e., we have

$$\frac{1}{3} \leq \nu < \frac{1}{2}.$$

Similarly, we have for hexagons

$$\frac{1}{4} \leq \nu < \frac{1}{2},$$

and for stripes

$$0 \leq \nu < \frac{1}{2}.$$

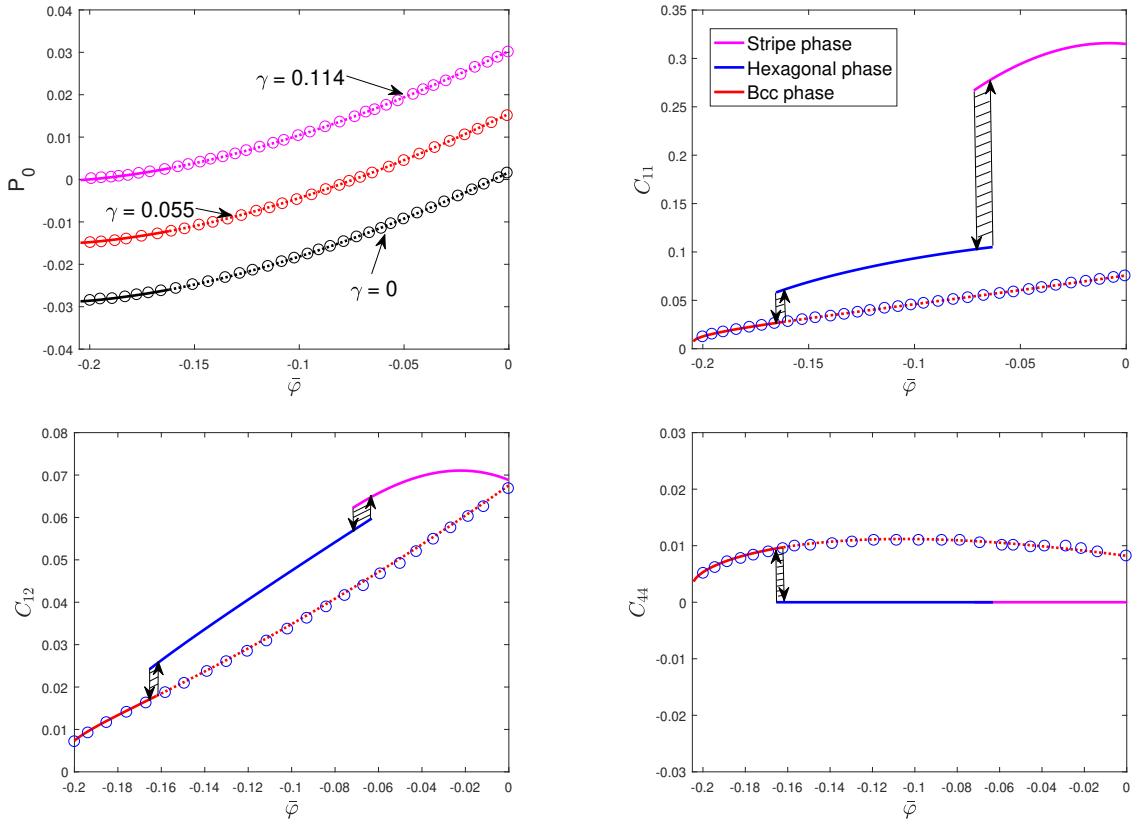

FIG. 9: Comparison between the results obtained in the present work and the ones obtained in [1]. The circles correspond to the results obtained in [1] whilst the solid and dash lines correspond to the results obtained in the present work. Observe that the results agree in the Bcc phase but differ elsewhere since [1] does not take account of the effect of phase transitions. $\epsilon = 0.0923$, $\tilde{\rho}_0 = 0.251$. Upper left: Pressure; upper right: C_{11}; lower left: C_{12}; lower right: C_{44}.

We show in Figure 11 the Poisson's ratio regarding the phase transition. Furthermore, we compare the results of the present work with the ones of [1] for the Poisson's ratio. See Figure 12.

VI. CONCLUSIONS

The main goal of the current work is to demonstrate that the PFC approach naturally gives rise to elastic constants which exhibit multi-valued behaviour across phase transitions. In order to readily facilitate comparison with previous work [1], we adopt the same basic setting. Namely, we confine our attention to the basic free energy functional considered in [1] in conjunction with consideration of simple one-mode approximations of the states. If one restricts attention to the body centered cubic state, then our formulae are in agreement with the numerical results presented in [1] across the full range. However, if one takes account of multiple states, the results differ in those regions where the Bcc state is not energetically favourable.

Interestingly, if one restricts attention to 2D states (by excluding the Bcc phase) then one may interpret the results as corresponding to a plane strain condition for which the Poisson ratio was shown in [16] to take the value $\nu = 1/4$. The dotted line shown in Figure 11 corresponds to excluding the Bcc phase and shows that the resulting values of the Poisson ratio lie in the range $[1/4, 1/2)$, consistent with the findings of [16]. Furthermore, one can, at least in principle, restrict to a univariate state by considering only the stripe state. Whilst no regular solid materials have a such a 3D rod-like structure, block copolymers [17, Figure 4] do exhibit these kinds of 3D rod-like structures and our results may find application to such materials.

In principle there is no difficulty in extending the analysis to include other 3D states besides Bcc considered here. However, our main objective here is to provide a clear comparison with the results presented in reference [1], where only the Bcc state is primarily considered. Likewise, one could generalize the approach to two-mode expansions. While the current work focuses on obtaining expressions for the elastic constants based on expressions for the state variable, one could follow [18] and attempt to

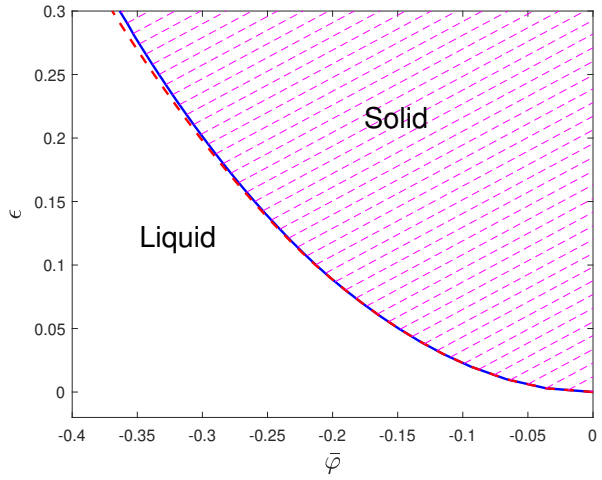

FIG. 10: Sign of the coefficient a defined in equations (35)-(37) with temperature and density. The red dashed line indicates the separation between the liquid and solid phases considered above. The coefficient a is non-negative in the hatched region.

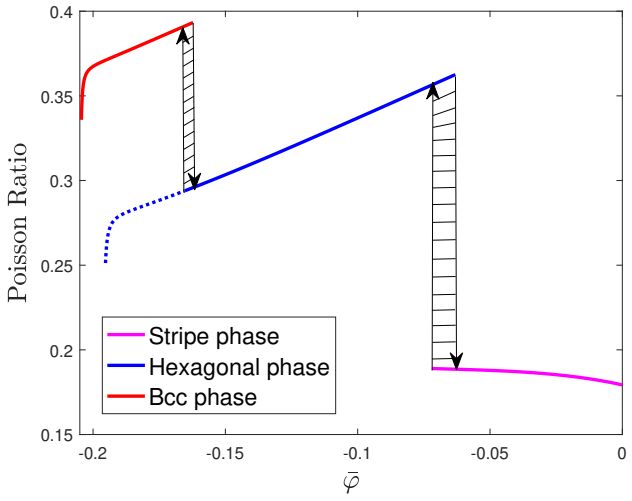

FIG. 11: Variation of the Poisson's ratio ν against the average of the density $\bar{\varphi}$. $\epsilon = 0.0923$, $\tilde{\rho}_0 = 0.251$. The dashed line shows the corresponding results if one excludes the Bcc state leaving only 2D states corresponding to plane strain conditions. Observe that the resulting Poisson's ratio lies in the range $[1/4, 1/2)$ consistent with the findings of [16].

derive analytic expressions for strain components across phase transitions.

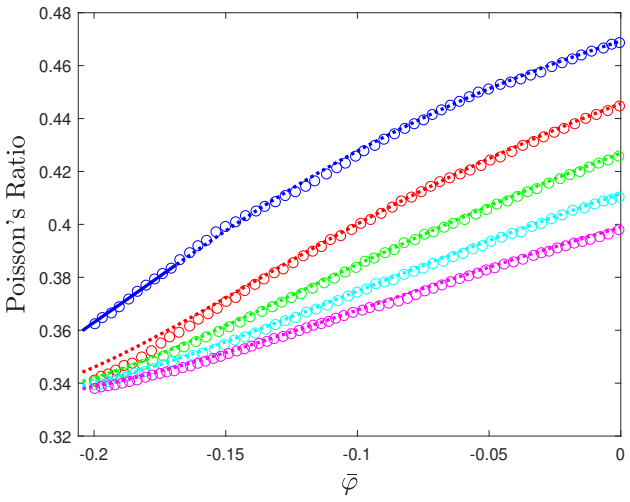

FIG. 12: Poisson's ratio ν against the average of the density $\bar{\varphi}$ for $\epsilon = 0.1$, 0.2, 0.3, 0.4, 0.5 (from top to bottom) and $\tilde{\rho}_0 = 0.251$. The results corresponding to solid and dash lines are the results of the present work whilst the ones corresponding to the symbol circles are the results of the work in [1].

Appendix: Calculation of the elastic constants for stripes, hexagons and Bcc

In this appendix, we present the calculation of the analytic forms of the elastic constants. Before doing this, let us first compute the value of partial derivatives of the average of the strained state with respect to the strain at the limit of vanishing strain, i.e., $\frac{\partial \bar{\varphi}_{\boldsymbol{\varepsilon}}}{\partial \varepsilon_{ii}}\Big|_{\boldsymbol{\varepsilon}=0}$ and $\frac{\partial^2 \bar{\varphi}_{\boldsymbol{\varepsilon}}}{\partial \varepsilon_{ii}\partial \varepsilon_{jj}}\Big|_{\boldsymbol{\varepsilon}=0}$. By using equations (3) and (4) and noting that

$$\begin{aligned} |\Omega_{\boldsymbol{\varepsilon}}| &= det[\boldsymbol{I}+\boldsymbol{\varepsilon}]\cdot|\Omega_0| \\ &= |\Omega_0|\left(1+\sum_i \varepsilon_{ii} + \frac{1}{2}\sum_{i,j}\left(\varepsilon_{ii}\varepsilon_{jj} - \varepsilon_{ij}\varepsilon_{ji} + O(\boldsymbol{\varepsilon}^3)\right)\right), \end{aligned} \tag{A.1}$$

we have

$$\begin{aligned} \frac{\partial \bar{\varphi}_{\boldsymbol{\varepsilon}}}{\partial \varepsilon_{ii}}\Big|_{\boldsymbol{\varepsilon}=0} &= (\bar{\varphi}_0+\tilde{\rho}_0)\frac{\partial\left(det^{-1}[\boldsymbol{I}+\boldsymbol{\varepsilon}]\right)}{\partial \varepsilon_{ii}}\Big|_{\boldsymbol{\varepsilon}=0} \\ &= -(\bar{\varphi}_0+\tilde{\rho}_0), \end{aligned} \tag{A.2}$$

and

$$\begin{aligned} \frac{\partial^2 \bar{\varphi}_{\boldsymbol{\varepsilon}}}{\partial \varepsilon_{ii}\partial \varepsilon_{jj}}\Big|_{\boldsymbol{\varepsilon}=0} &= (\bar{\varphi}_0+\tilde{\rho}_0)\frac{\partial^2\left(det^{-1}[\boldsymbol{I}+\boldsymbol{\varepsilon}]\right)}{\partial \varepsilon_{ii}\partial \varepsilon_{jj}}\Big|_{\boldsymbol{\varepsilon}=0} \\ &= \begin{cases} 2(\bar{\varphi}_0+\tilde{\rho}_0), & \text{if } i=j, \\ \bar{\varphi}_0+\tilde{\rho}_0, & \text{if } i\neq j. \end{cases} \end{aligned} \tag{A.3}$$

We first consider the case of zero shear strain, i.e., $\varepsilon_{ij} = 0$ for $i \neq j$. In this case, we can compute the pre-existing

pressure P_0 and the elastic constants C_{11}, C_{12}. We begin by compute the free energy of the strained state. By substituting the following strained solution

$$\varphi_{\boldsymbol{\varepsilon}}(\boldsymbol{r}) = \bar{\varphi}_{\boldsymbol{\varepsilon}} + \sum_{\boldsymbol{K}_{\boldsymbol{\varepsilon}}} A_{\boldsymbol{K}_{\boldsymbol{\varepsilon}}} e^{\mathrm{i}\boldsymbol{K}_{\boldsymbol{\varepsilon}}\cdot\boldsymbol{r}}$$

into the free energy functional (1), we obtain the total free energy of the strained state

$$F_{\boldsymbol{\varepsilon}} = |\Omega_0| \cdot det[\boldsymbol{I}+\boldsymbol{\varepsilon}] f_{\boldsymbol{\varepsilon}}, \tag{A.4}$$

where

$$f_{\boldsymbol{\varepsilon}} = f^0_{\boldsymbol{\varepsilon}} + f^1_{\boldsymbol{\varepsilon}} + O(\boldsymbol{\varepsilon}^3) \tag{A.5}$$

is the free energy density of the strained state with $f^0_{\boldsymbol{\varepsilon}}$ and $f^1_{\boldsymbol{\varepsilon}}$ being given by

$$f^0_{\boldsymbol{\varepsilon}} = f_s(\bar{\varphi}_{\boldsymbol{\varepsilon}}, A^{\boldsymbol{\varepsilon}}_s),\ f^1_{\boldsymbol{\varepsilon}} = 4\varepsilon^2_{11}(A^{\boldsymbol{\varepsilon}}_s)^2 \tag{A.6}$$

for stripes, or

$$f^0_{\boldsymbol{\varepsilon}} = f_h(\bar{\varphi}_{\boldsymbol{\varepsilon}}, A^{\boldsymbol{\varepsilon}}_h),\ f^1_{\boldsymbol{\varepsilon}} = \left(\frac{9}{2}(\varepsilon^2_{11}+\varepsilon^2_{22}) + 3\varepsilon_{11}\varepsilon_{22}\right)(A^{\boldsymbol{\varepsilon}}_h)^2 \tag{A.7}$$

for hexagons, or

$$\begin{aligned} f^0_{\boldsymbol{\varepsilon}} &= f_b(\bar{\varphi}_{\boldsymbol{\varepsilon}}, A^{\boldsymbol{\varepsilon}}_b), \\ f^1_{\boldsymbol{\varepsilon}} &= \left(4\sum_{i=1}^{3}\varepsilon^2_{ii} + 2\sum_{i,j=1,i\neq j}^{3}\varepsilon_{ii}\varepsilon_{jj}\right)(A^{\boldsymbol{\varepsilon}}_b)^2 \end{aligned} \tag{A.8}$$

for Bcc, where the forms of $f_s(\bar{\varphi}_{\boldsymbol{\varepsilon}}, A^{\boldsymbol{\varepsilon}}_s)$, $f_h(\bar{\varphi}_{\boldsymbol{\varepsilon}}, A^{\boldsymbol{\varepsilon}}_h)$ and $A^{\boldsymbol{\varepsilon}}_h)$ and $f_b(\bar{\varphi}_{\boldsymbol{\varepsilon}}, A^{\boldsymbol{\varepsilon}}_b)$ are given by (13), (15) and (16), respectively. Minimizing the strained free energy yields the amplitudes of the strained stripe, hexagon and Bcc states given by

$$\begin{aligned} A^{\boldsymbol{\varepsilon}}_s &= \pm\sqrt{(\epsilon - 3\bar{\varphi}^2 - 4\varepsilon^2_{11})/3}, \\ A^{\boldsymbol{\varepsilon}}_h &= -\bar{\varphi}/5 \\ &\quad \pm\sqrt{15\epsilon - 36\bar{\varphi}^2 - 15(3(\varepsilon^2_{11}+\varepsilon^2_{22})/2 - \varepsilon_{11}\varepsilon_{22})}\Big/15 \end{aligned}$$

and

$$\begin{aligned} A^{\boldsymbol{\varepsilon}}_b &= -2\bar{\varphi}/15 \\ &\pm\frac{1}{15}\sqrt{5\epsilon - 11\bar{\varphi}^2 - 5\Big(2\sum_{i=1}^{3}\varepsilon^2_{ii} + \sum_{i,j=1,i\neq j}^{3}\varepsilon_{ii}\varepsilon_{jj}\Big)\Big/3}. \end{aligned}$$

Note that here we omit the high order term with respect to the strain. Correspondingly, by using the above three equations, we can obtain the first-order derivative of the stained amplitudes with respect to the stain, i.e.,

$$\frac{\partial A^{\boldsymbol{\varepsilon}}_{\diamondsuit}}{\partial\varepsilon_{ii}}\Big|_{\boldsymbol{\varepsilon}=0}, \tag{A.9}$$

where $\diamondsuit$ can be 's', 'h' or 'b' for the stripes, hexagons or Bcc.

We now compute the pre-existed pressure P_0 and the elastic constant C_{11}, C_{12}. To this end, by the definition of the pressure, i.e., equation (19), and (A.4), we have

$$\begin{aligned} P_0 &= -\left(\frac{\partial\, det[\boldsymbol{I}+\boldsymbol{\varepsilon}]}{\partial\varepsilon_{ii}} f_{\boldsymbol{\varepsilon}} + det[\boldsymbol{I}+\boldsymbol{\varepsilon}]\frac{\partial f_{\boldsymbol{\varepsilon}}}{\partial\varepsilon_{ii}}\right)\Big|_{\boldsymbol{\varepsilon}=0} \\ &= -\left(f_{\boldsymbol{\varepsilon}} + \frac{\partial f_{\boldsymbol{\varepsilon}}}{\partial A^{\boldsymbol{\varepsilon}}}\frac{\partial A^{\boldsymbol{\varepsilon}}}{\partial\varepsilon_{ii}} + \frac{\partial f_{\boldsymbol{\varepsilon}}}{\partial\bar{\varphi}_{\boldsymbol{\varepsilon}}}\frac{\partial\bar{\varphi}_{\boldsymbol{\varepsilon}}}{\partial\varepsilon_{ii}}\right)\Big|_{\boldsymbol{\varepsilon}=0}, \end{aligned}$$

where $f_{\boldsymbol{\varepsilon}}$ is given by (A.5) and $A^{\boldsymbol{\varepsilon}}$ can be $A^{\boldsymbol{\varepsilon}}_s$, $A^{\boldsymbol{\varepsilon}}_h$ or $A^{\boldsymbol{\varepsilon}}_b$. Since $A^{\boldsymbol{\varepsilon}}$ is a minimum of $f_{\boldsymbol{\varepsilon}}$, we then have

$$\frac{\partial f_{\boldsymbol{\varepsilon}}}{\partial A^{\boldsymbol{\varepsilon}}} = 0. \tag{A.10}$$

Using the above two equations gives

$$P_0 = -\left(f_{\boldsymbol{\varepsilon}} + \frac{\partial f_{\boldsymbol{\varepsilon}}}{\partial\bar{\varphi}_{\boldsymbol{\varepsilon}}}\frac{\partial\bar{\varphi}_{\boldsymbol{\varepsilon}}}{\partial\varepsilon_{ii}}\right)\Big|_{\boldsymbol{\varepsilon}=0}. \tag{A.11}$$

Thus, by using the above equation and (A.2), and equations (A.6)-(A.8), we can obtain the pre-existed pressures for stripes, and hexagons and Bcc, i.e., equations (24), (27) and (30).

For the elastic constants C_{11}, we have from (18), (20), (A.1) and (A.4) that

$$\begin{aligned} C_{11} :=& C_{1111} = \frac{\partial^2\left(det[\boldsymbol{I}+\boldsymbol{\varepsilon}] f_{\boldsymbol{\varepsilon}} + P_0|\Omega_{\boldsymbol{\varepsilon}}|/|\Omega_0|\right)}{\partial\varepsilon^2_{11}}\Big|_{\boldsymbol{\varepsilon}=0} \\ =& \Big(\frac{\partial^2\, det[\boldsymbol{I}+\boldsymbol{\varepsilon}]}{\partial\varepsilon^2_{11}} f_{\boldsymbol{\varepsilon}} + 2\frac{\partial\, det[\boldsymbol{I}+\boldsymbol{\varepsilon}]}{\partial\varepsilon_{11}}\frac{\partial f_{\boldsymbol{\varepsilon}}}{\partial\varepsilon_{11}} \\ &+ det[\boldsymbol{I}+\boldsymbol{\varepsilon}]\frac{\partial^2 f_{\boldsymbol{\varepsilon}}}{\partial\varepsilon^2_{11}}\Big)\Big|_{\boldsymbol{\varepsilon}=0}. \end{aligned}$$

Using (A.1) again, we have that as $\boldsymbol{\varepsilon}\to 0$,

$$C_{11} = 2\frac{\partial f_{\boldsymbol{\varepsilon}}}{\partial\varepsilon_{11}} + \frac{\partial^2 f_{\boldsymbol{\varepsilon}}}{\partial\varepsilon^2_{11}} = 2\frac{\partial f_{\boldsymbol{\varepsilon}}}{\partial\bar{\varphi}_{\boldsymbol{\varepsilon}}}\frac{\partial\bar{\varphi}_{\boldsymbol{\varepsilon}}}{\partial\varepsilon_{11}} + \frac{\partial^2 f^0_{\boldsymbol{\varepsilon}}}{\partial\varepsilon^2_{11}} + \frac{\partial^2 f^1_{\boldsymbol{\varepsilon}}}{\partial\varepsilon^2_{11}}. \tag{A.12}$$

Using the chain rule and equation (A.10), we have

$$\begin{aligned} \frac{\partial^2 f^0_{\boldsymbol{\varepsilon}}}{\partial\varepsilon^2_{11}} &= \frac{\partial A^{\boldsymbol{\varepsilon}}}{\partial\varepsilon_{11}}\left(\frac{\partial^2 f^0_{\boldsymbol{\varepsilon}}}{\partial(A^{\boldsymbol{\varepsilon}})^2}\frac{\partial A^{\boldsymbol{\varepsilon}}}{\partial\varepsilon_{11}} + \frac{\partial^2 f^0_{\boldsymbol{\varepsilon}}}{\partial A^{\boldsymbol{\varepsilon}}\partial\bar{\varphi}_{\boldsymbol{\varepsilon}}}\frac{\partial\bar{\varphi}_{\boldsymbol{\varepsilon}}}{\partial\varepsilon_{11}}\right) \\ &+ \frac{\partial\bar{\varphi}_{\boldsymbol{\varepsilon}}}{\partial\varepsilon_{11}}\left(\frac{\partial^2 f^0_{\boldsymbol{\varepsilon}}}{\partial\bar{\varphi}_{\boldsymbol{\varepsilon}}\partial A^{\boldsymbol{\varepsilon}}}\frac{\partial A^{\boldsymbol{\varepsilon}}}{\partial\varepsilon_{11}} + \frac{\partial^2 f^0_{\boldsymbol{\varepsilon}}}{\partial(\bar{\varphi}_{\boldsymbol{\varepsilon}})^2}\frac{\partial\bar{\varphi}_{\boldsymbol{\varepsilon}}}{\partial\varepsilon_{11}}\right) + \frac{\partial f^0_{\boldsymbol{\varepsilon}}}{\partial\bar{\varphi}_{\boldsymbol{\varepsilon}}}\frac{\partial^2\bar{\varphi}_{\boldsymbol{\varepsilon}}}{\partial\varepsilon^2_{11}} \end{aligned} \tag{A.13}$$

as $\boldsymbol{\varepsilon}\to 0$. We now show that the first parentheses of the right hand side of the above equation vanishes as $\boldsymbol{\varepsilon}\to 0$. We only show the case of Bcc, for the cases of stripe and hexagon, the arguments are similar. To this end, by equation (A.10), we have

$$\epsilon - 3\bar{\varphi}^2_{\boldsymbol{\varepsilon}} - 12\bar{\varphi}_{\boldsymbol{\varepsilon}}A^{\boldsymbol{\varepsilon}}_b - 45(A^{\boldsymbol{\varepsilon}}_b)^2 + \frac{1}{A^{\boldsymbol{\varepsilon}}_b}\frac{\partial f^1_{\boldsymbol{\varepsilon}}}{\partial A^{\boldsymbol{\varepsilon}}_b} = 0,$$

where $f^1_{\boldsymbol{\varepsilon}}$ is given in (A.8). By differentiating the above equation with respect to ε_{11} and taking the limit as $\boldsymbol{\varepsilon}\to 0$, we have

$$(2\bar{\varphi}_{\boldsymbol{\varepsilon}} + 15A^{\boldsymbol{\varepsilon}}_b)\frac{\partial A^{\boldsymbol{\varepsilon}}_b}{\partial\varepsilon_{11}}\Big|_{\boldsymbol{\varepsilon}=0} = -(\bar{\varphi}_{\boldsymbol{\varepsilon}} + 2A^{\boldsymbol{\varepsilon}}_b)\frac{\partial\bar{\varphi}_{\boldsymbol{\varepsilon}}}{\partial\varepsilon_{11}}\Big|_{\boldsymbol{\varepsilon}=0}. \tag{A.14}$$

By the virtue of the above two equations and (A.8), we have that

$$\left(\frac{\partial^2 f^0_{\boldsymbol{\varepsilon}}}{\partial (A^{\boldsymbol{\varepsilon}})^2}\frac{\partial A^{\boldsymbol{\varepsilon}}}{\partial \varepsilon_{11}} + \frac{\partial^2 f^0_{\boldsymbol{\varepsilon}}}{\partial A^{\boldsymbol{\varepsilon}}\partial \bar{\varphi}_{\boldsymbol{\varepsilon}}}\frac{\partial \bar{\varphi}_{\boldsymbol{\varepsilon}}}{\partial \varepsilon_{11}}\right)\Big|_{\boldsymbol{\varepsilon}=0} = 0.$$

Thus, as $\boldsymbol{\varepsilon} \to 0$, the equation (A.13) becomes

$$\begin{aligned}\frac{\partial^2 f^0_{\boldsymbol{\varepsilon}}}{\partial \varepsilon_{11}^2} =& \frac{\partial \bar{\varphi}_{\boldsymbol{\varepsilon}}}{\partial \varepsilon_{11}}\left(\frac{\partial^2 f^0_{\boldsymbol{\varepsilon}}}{\partial \bar{\varphi}_{\boldsymbol{\varepsilon}}\partial A^{\boldsymbol{\varepsilon}}}\frac{\partial A^{\boldsymbol{\varepsilon}}}{\partial \varepsilon_{11}} + \frac{\partial^2 f^0_{\boldsymbol{\varepsilon}}}{\partial (\bar{\varphi}_{\boldsymbol{\varepsilon}})^2}\frac{\partial \bar{\varphi}_{\boldsymbol{\varepsilon}}}{\partial \varepsilon_{11}}\right)\\ &+ \frac{\partial f^0_{\boldsymbol{\varepsilon}}}{\partial \bar{\varphi}_{\boldsymbol{\varepsilon}}}\frac{\partial^2 \bar{\varphi}_{\boldsymbol{\varepsilon}}}{\partial \varepsilon_{11}^2}.\end{aligned} \tag{A.15}$$

Furthermore, we have from equations (A.2) and (A.3) that

$$\left(\frac{\partial f^0_{\boldsymbol{\varepsilon}}}{\partial \bar{\varphi}_{\boldsymbol{\varepsilon}}}\frac{\partial^2 \bar{\varphi}_{\boldsymbol{\varepsilon}}}{\partial \varepsilon_{11}^2} + 2\frac{\partial f_{\boldsymbol{\varepsilon}}}{\partial \bar{\varphi}_{\boldsymbol{\varepsilon}}}\frac{\partial \bar{\varphi}_{\boldsymbol{\varepsilon}}}{\partial \varepsilon_{11}}\right)\Big|_{\boldsymbol{\varepsilon}=0} = 0. \tag{A.16}$$

Using equations (A.12), (A.15) and (A.16), we have that as $\boldsymbol{\varepsilon} \to 0$,

$$C_{11} = \frac{\partial \bar{\varphi}_{\boldsymbol{\varepsilon}}}{\partial \varepsilon_{11}}\left(\frac{\partial^2 f^0_{\boldsymbol{\varepsilon}}}{\partial \bar{\varphi}_{\boldsymbol{\varepsilon}}\partial A^{\boldsymbol{\varepsilon}}}\frac{\partial A^{\boldsymbol{\varepsilon}}}{\partial \varepsilon_{11}} + \frac{\partial^2 f^0_{\boldsymbol{\varepsilon}}}{\partial (\bar{\varphi}_{\boldsymbol{\varepsilon}})^2}\frac{\partial \bar{\varphi}_{\boldsymbol{\varepsilon}}}{\partial \varepsilon_{11}}\right) + \frac{\partial^2 f^1_{\boldsymbol{\varepsilon}}}{\partial \varepsilon_{11}^2}. \tag{A.17}$$

Then, we can obtain the elastic constants C_{11} for stripes, hexagons and Bcc, i.e., (25), (28) and (31), by the above equation and equations (A.2), (A.3), (A.6)-(A.8).

Similarly, we can obtain the elastic constant

$$C_{12} = \Big(f_{\boldsymbol{\varepsilon}} + \frac{\partial f_{\boldsymbol{\varepsilon}}}{\partial \bar{\varphi}_{\boldsymbol{\varepsilon}}}\sum_{i=1,2}\frac{\partial \bar{\varphi}_{\boldsymbol{\varepsilon}}}{\partial \varepsilon_{ii}} + \frac{\partial^2 (f^0_{\boldsymbol{\varepsilon}} + f^1_{\boldsymbol{\varepsilon}})}{\partial \varepsilon_{11}\partial \varepsilon_{22}}\Big)\Big|_{\boldsymbol{\varepsilon}=0} + P_0$$

with

$$\begin{aligned}\frac{\partial^2 f^0_{\boldsymbol{\varepsilon}}}{\partial \varepsilon_{11}\partial \varepsilon_{22}} =& \frac{\partial \bar{\varphi}_{\boldsymbol{\varepsilon}}}{\partial \varepsilon_{11}}\left(\frac{\partial^2 f^0_{\boldsymbol{\varepsilon}}}{\partial \bar{\varphi}_{\boldsymbol{\varepsilon}}\partial A^{\boldsymbol{\varepsilon}}}\frac{\partial A^{\boldsymbol{\varepsilon}}}{\partial \varepsilon_{22}} + \frac{\partial^2 f^0_{\boldsymbol{\varepsilon}}}{\partial (\bar{\varphi}_{\boldsymbol{\varepsilon}})^2}\frac{\partial \bar{\varphi}_{\boldsymbol{\varepsilon}}}{\partial \varepsilon_{22}}\right)\\ &+ \frac{\partial f^0_{\boldsymbol{\varepsilon}}}{\partial \bar{\varphi}_{\boldsymbol{\varepsilon}}}\frac{\partial^2 \bar{\varphi}_{\boldsymbol{\varepsilon}}}{\partial \varepsilon_{11}\partial \varepsilon_{22}}.\end{aligned}$$

Moreover, we have

$$\left(\frac{\partial f^0_{\boldsymbol{\varepsilon}}}{\partial \bar{\varphi}_{\boldsymbol{\varepsilon}}}\frac{\partial^2 \bar{\varphi}_{\boldsymbol{\varepsilon}}}{\partial \varepsilon_{11}\partial \varepsilon_{22}} + \frac{\partial f_{\boldsymbol{\varepsilon}}}{\partial \bar{\varphi}_{\boldsymbol{\varepsilon}}}\frac{\partial \bar{\varphi}_{\boldsymbol{\varepsilon}}}{\partial \varepsilon_{22}}\right)\Big|_{\boldsymbol{\varepsilon}=0} = 0.$$

Using the above three equations and (A.11) gives that as $\boldsymbol{\varepsilon} \to 0$,

$$C_{12} = \frac{\partial \bar{\varphi}_{\boldsymbol{\varepsilon}}}{\partial \varepsilon_{11}}\left(\frac{\partial^2 f^0_{\boldsymbol{\varepsilon}}}{\partial \bar{\varphi}_{\boldsymbol{\varepsilon}}\partial A^{\boldsymbol{\varepsilon}}}\frac{\partial A^{\boldsymbol{\varepsilon}}}{\partial \varepsilon_{22}} + \frac{\partial^2 f^0_{\boldsymbol{\varepsilon}}}{\partial (\bar{\varphi}_{\boldsymbol{\varepsilon}})^2}\frac{\partial \bar{\varphi}_{\boldsymbol{\varepsilon}}}{\partial \varepsilon_{22}}\right) + \frac{\partial^2 f^1_{\boldsymbol{\varepsilon}}}{\partial \varepsilon_{11}\partial \varepsilon_{22}}. \tag{A.18}$$

Then we obtain the elastic constants C_{12} for hexagons and Bcc, i.e., (29) and (32), by the above equation and (A.2), (A.3), (A.6)-(A.8).

The elastic constant $C_{44} := C_{2323}$ can be obtained by using a similar argument as that for C_{11} and C_{12}. To this end, we let all components of the strain $\boldsymbol{\varepsilon}$ be zero except ε_{23} and ε_{32}. The resulting expression for the elastic constant C_{44} is given by

$$C_{44} = \frac{\partial^2 f^1_{\boldsymbol{\varepsilon}}}{\partial \varepsilon_{23}^2}, \tag{A.19}$$

where $f^1_{\boldsymbol{\varepsilon}}$ in this case is given by

$$f^1_{\boldsymbol{\varepsilon}} = \begin{cases} O(\boldsymbol{\varepsilon}^4), \text{ for stripes or hexagons,} \\ 2(\varepsilon_{23}+\varepsilon_{32})^2 (A^{\boldsymbol{\varepsilon}}_b)^2 + O(\boldsymbol{\varepsilon}^4), \text{ for Bcc} \end{cases}$$

with

$$A^{\boldsymbol{\varepsilon}}_b = -\frac{2}{15}\bar{\varphi} \pm \frac{1}{15}\sqrt{5\epsilon - 11\bar{\varphi}^2 - \frac{(\varepsilon_{23}+\varepsilon_{32})^2}{3}}.$$

Thus, C_{44} for stripes or hexagons vanishes whilst C_{44} for Bcc is given by (33).

[1] Z.-L. Wang, Z.-F. Huang, and Z. Liu, Physical Review B **97**, 144112 (2018).
[2] K. Elder, M. Katakowski, M. Haataja, and M. Grant, Physical review letters **88**, 245701 (2002).
[3] K. Elder and M. Grant, Physical Review E **70**, 051605 (2004).
[4] F. Willis, R. Leisure, and T. Kanashiro, Physical Review B **54**, 9077 (1996).
[5] A. Jaatinen, C. Achim, K. Elder, and T. Ala-Nissila, Physical Review E **80**, 031602 (2009).
[6] M. C. Cross and P. C. Hohenberg, Reviews of modern physics **65**, 851 (1993).
[7] A. Karma, Bulletin of the American Physical Society **58** (2013).
[8] H. Emmerich, H. Löwen, R. Wittkowski, T. Gruhn, G. I. Tóth, G. Tegze, and L. Gránásy, Advances in Physics **61**, 665 (2012).
[9] D. J. Lloyd, B. Sandstede, D. Avitabile, and A. R. Champneys, SIAM Journal on Applied Dynamical Systems **7**, 1049 (2008).
[10] K.-A. Wu and A. Karma, Physical Review B **76**, 184107 (2007).
[11] C. W. David, Chemistry Education Materials **89** (2015).
[12] J. Atteberry, D. Agosta, C. Nattrass, R. Leisure, I. Jacob, R. Bowman Jr, and O. Yeheskel, Journal of alloys and compounds **376**, 139 (2004).
[13] D. Agosta, J. Hightower, K. Foster, R. Leisure, and Z. Gavra, Journal of alloys and compounds **346**, 1 (2002).
[14] J. Atteberry, D. Agosta, R. Leisure, O. Beeri, and M. Mintz, Journal of alloys and compounds **365**, 68

(2004).
[15] G. Quirion, M. Abu-Kharma, I. Sergienko, M. Bromberek, M. Clouter, and B. Mroz, Journal of Physics: Condensed Matter **15**, 4979 (2003).
[16] A. Skaugen, L. Angheluta, and J. Viñals, Physical Review B **97**, 054113 (2018).
[17] A.-V. Ruzette and L. Leibler, Nature materials **4**, 19 (2005).
[18] M. Salvalaglio, A. Voigt, and K. R. Elder, npj Computational Materials **5**, 48 (2019).